Deuterium isotope effect on the oxidation of monophenols and *o*-diphenols by tyrosinase

Lorena G. FENOLL*, María José PEÑALVER*, José N. RODRÍGUEZ-LÓPEZ*, P. A. GARCÍA-RUIZ†, Francisco GARCÍA-CÁNOVAS*[1] and José TUDELA*

*GENZ (Grupo de Investigación de Enzimología), Departamento de Bioquímica y Biología Molecular-A, Facultad de Biología, Universidad de Murcia, A. Correos 4021, E-30080, Murcia, Spain, and ‡Departamento de Química Orgánica, Facultad de Química, Universidad de Murcia, A. Correos 4021. E-30080 Murcia, Spain

A solvent deuterium isotope effect on the catalytic affinity (k_m) and catalytic constant (k_{cat}) of tyrosinase in its action on different monophenols and *o*-diphenols was observed. The catalytic constant decreased in all substrates as the molar fraction of deuterated water in the medium increased, while the catalytic affinity only decreased for the *o*-diphenols with an R group in C-1 [-H, -CH_3 and -$CH(CH_3)_2$]. In a proton inventory study of the oxidation of *o*-diphenols, the representation of $k_{cat}^{fn}/k_{cat}^{f0}$ against *n* (atom fractions of deuterium), where k_{cat}^{fn} is the catalytic constant for a molar fraction of deuterium (*n*) and k_{cat}^{f0} is the corresponding kinetic parameter in a water solution, was linear for all substrates, indicating that only one of the four protons transferred from the hydroxy groups of the two molecules of substrate, which are oxidized in one turnover, is responsible for the isotope effects, the proton transferred from the hydroxy group of C-4 to the peroxide of the *oxy*tyrosinase form (E_{ox}). However, in the representation of K_m^{fn}/K_m^{f0} against *n*, where K_m^{fn} represents the catalytic affinity for a molar fraction of deuterium (*n*) and K_m^{f0} is the corresponding kinetic parameter in a water solution, a linear decrease was observed as *n* increased in the case of *o*-diphenols with the R group [-H, -CH_3 and -$CH(CH_3)_2$], and a parabolic increase with other R groups, indicating that more than one proton is responsible for the isotope effects on substrate binding. In the case of monophenols with six protons transferred in the catalytic cycle, the isotope effect occurs in the same way as for *o*-diphenols. In the present paper, the fractionation factors of different monophenols and *o*-diphenols are described and possible mechanistic implications are discussed.

Key words: deuterium isotope effect, diphenols, monophenols, mushroom, polyphenol oxidase, tyrosinase.

INTRODUCTION

Tyrosinase or polyphenol oxidase (monophenol, *o*-diphenol: oxygen oxidoreductase, EC 1.14.18.1) is a copper-containing enzyme that is widely distributed throughout nature. It is of central importance in such processes as vertebrate pigmentation and the browning of fruits and vegetables [1,2]. The tyrosinases isolated from several different sources have similar structural and functional characteristics [3,4]. Tyrosinases catalyse two type of reactions, the o-hydroxylation of monophenols (monophenolase activity) and the oxidation of *o*-diphenols to *o*-quinones (diphenolase activity) using molecular oxygen [5]. The catalytic cycles for the monophenolase and diphenolase activities are coupled not only to each other, but also to non-enzymic reactions involving the *o*-quinone products [6–8].

In button mushroom (*Agaricus bisporus*) tyrosinase (M_r 11.2 × 10^4) [9], *met* (E_m, Cu^{2+} Cu^{2+}), *deoxy* (E_d, Cu^{+} Cu^{+}), and *oxy* (E_{ox}, Cu^{2+} Cu^{2+} O_2^{2-}) forms have been identified during the catalytic cycle [10,11]. Previous studies have looked at the kinetic mechanism of the enzyme's action on monophenols and *o*-diphenols [6,8,12–14] or the influence of the stability of the *o*-quinones generated on the enzyme's behaviour towards monophenols [15]. In these studies, the strength of the nucleophilic attack of the OH in the C-4 position was seen to be a determining factor in the case of monophenols [14] and, to a certain extent, in the case of *o*-diphenols [11,14,16].

The kinetic mechanism of the enzyme acting on monophenols and *o*-diphenols is depicted in Scheme 1. In the oxidase cycle, the reaction mechanism described suggests that when the *o*-diphenol binds to the E_m form of tyrosinase (Scheme 2), a proton is transferred from the OH of C-4 to a base (B) near Cu_A, while a second proton from the OH of C-3 is transferred to the histidine bound to Cu_B [16,17]. Both protonic transfers occur from oxygen to nitrogen and accompany the nucleophilic attack of the oxygen atoms on their respective Cu_A and Cu_B [11]. However, during the binding of the substrate to the E_{ox} form, the proton from the OH of C-4 is probably transferred to the peroxide bound to the copper atoms (proton transfer from oxygen to oxygen) and the hydroxyl proton of C-3 to the histidine bound to Cu_B (proton transfer from oxygen to nitrogen) [16,18]. In both cases, the nucleophilic attack of the oxygen atoms on the copper atoms of the binuclear site is accompanied by proton transfer. Therefore, during the catalytic cycle of the diphenolase activity of the enzyme, four proton-transfer processes take place, three from the oxygen atoms of the hydroxy groups (of C-4 and C-3) (Scheme 2) to nitrogen atoms of histidine residues, and the fourth to one oxygen atom of the peroxide group on Cu_A and Cu_B.

When the enzyme acts on monophenols (monophenolase cycle), *o*-diphenol is accumulated in the reaction medium, and two steps occur (Scheme 2) in addition to the proton transfers described above for the oxidation of *o*-diphenols: the dead-end pathway, in which M binds to E_m, transferring a proton to the nitrogen atom of the base (B) (probably histidine) near Cu_A, and M binds to E_{ox} (beginning of monophenolase cycle), transferring a proton to the peroxide group bound to the copper atoms at the equatorial plane (protonic transfer between oxygen atoms). In a

Abbreviations used: DHPAA, dihydroxyphenylacetic acid; DHPPA, dihydroxyphenylpropionic acid; 4EP, 4-ethoxyphenol; 3HA, 3-hydroxyanisole; 4HA, 4-hydroxyanisole; 3HBA, 3-hydroxybenzylalcohol; 4HBA, 4-hydroxybenzylalcohol; 4MC, 4-methylcatechol; MBTH, 3-methyl-2-benzothiazolinone hydrazone; PHPAA, *p*-hydroxyphenylacetic acid; PHPPA, *p*-hydroxyphenylpropionic acid; TBC, 4-*tert*-butylcatechol.

[1] To whom correspondence should be addressed (e-mail canovasf@um.es).

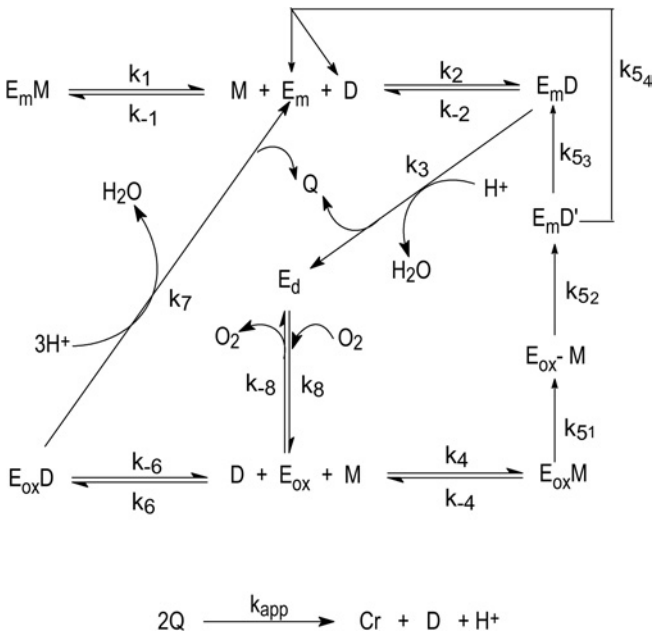

Scheme 1 Reaction mechanism of tyrosinase acting on monophenols and diphenols with the chemical reactions corresponding to quinone evolution

E_d is converted into E_{ox} by binding oxygen (O_2). E_{ox} can either react with a monophenol (M) or with a *o*-diphenol (D). In the first case, M evolves to D and may be oxidized to Q, generating E_d or be released into the medium, generating, in turn, E_m. If E_{ox} reacts with D, the corresponding Q is generated. E_m can oxidize D, generating Q, and be converted into E_d, and E_m may bind to M, generating the dead-end complex E_mM. Spontaneous endocyclization of Q gives rise to Cr and D.

previous study [14], we suggested that the slow step corresponded to the nucleophilic attack of the oxygen of the hydroxy group at the C-4 position of the benzene ring on the Cu_A atom of the enzyme active site, a proton being transferred to the peroxide oxygen at the same time (k_{5_1}, Scheme 2).

The aim of the present study was to obtain further evidence to support the above by means of a proton inventory study and to provide more information on the limiting step of the mechanism [19]. It was thought that if a single protonic site of an enzyme was engaged in proton transfer or in another form of protonic reorganization in the rate-determining step, and that if this process was responsible for the entire solvent isotope effect, then a linear ('one-proton') form of $k_{cat}^{f_n}/k_{cat}^{f_0}$ against n would be evident [19,20], where $k_{cat}^{f_n}$ is the catalytic constant for a molar fraction of deuterium (n) and $k_{cat}^{f_0}$ is the corresponding kinetic parameter in a water solution. At the same time, a non-linear dependence of $K_m^{f_n}/K_m^{f_0}$ against n would indicate that more than one proton was responsible for the isotope effect, where $K_m^{f_n}$ represents the catalytic affinity for a molar fraction of deuterium (n) and $K_m^{f_0}$ is the corresponding kinetic parameter in a water solution.

The solvent deuterium isotope effect on the activity of the tyrosinase enzyme has been described in the literature with a monophenol, L-tyrosine [18], and an *o*-diphenol, TBC (4-*tert*-butylcatechol) [20]. The investigation we describe in the present paper was intended to provide more information about the reaction mechanism of the enzyme, by studying monophenols with a cationic (tyramine), aninonic [PHPAA (*p*-hydroxyphenylacetic acid), PHPPA (*p*-hydroxyphenylpropionic acid)], zwitterionic with stereoisomers (L-tyrosine and DL-tyrosine) or uncharged [4HA (4-hydroxyanisole), 4EP (4-ethoxyphenol), 4HBA (4-hydroxybenzylalcohol)] R group on C-1, and some uncharged 3-monophenols [3HA (3-hydroxyanisole), 3HBA (3-hydroxybenzylalcohol)]. In the case of *o*-diphenols, we studied those with a cationic (dopamine), anionic [DHPPA (dihydroxyphenylpropionic acid), DHPAA (dihydroxyphenylacetic acid)], zwitterionic with stereoisomers (L-dopa, D-dopa, DL-dopa), and uncharged [4MC (4-methylcatechol), TBC, catechol] R group. From a study of the deuterium isotope effect on the binding and transformation constants, information about the reaction mechanism of tyrosinase on monophenols and *o*-diphenols was obtained.

MATERIALS AND METHODS

Reagents

TBC, catechol and 4MC were purchased from Fluka (Madrid, Spain); 4EP, 3HA and 4HA were from Aldrich (Madrid, Spain); DHPAA, DHPPA, L-dopa, DL-dopa, D-dopa, 3HBA, 4HBA, PHPAA, PHPPA, MBTH (3-methyl-2-benzothiazolinone hydrazone), DL-tyrosine and L-tyrosine were from Sigma (Madrid, Spain) and ^2H_2O (99.8 % ^2H) was obtained from Scharlau Chemie (Barcelona, Spain). Stock solutions of reducing substrate were prepared in 0.15 mM phosphoric acid in order to prevent autooxidation. All other chemicals were of analytical grade and supplied by Merck (Frankfurt, Germany). The acidic character of MBTH required the use of 50 mM buffer in the assay medium. To dissolve the MBTH-quinone adducts, 2 % (v/v) DMF (*N*,*N*′-dimethylformamide) was added to the assay medium [21,22]. Milli-Q system (Millipore Corp.) ultrapure water was used throughout this research.

Enzyme source

Mushroom tyrosinase (8300 units/mg) was purified by following Duckworth and Coleman's procedure [23], but with two additional chromatographic steps [17]. Protein concentrations were determined by using Bradford's method [24] using BSA as a standard.

Spectrophotometric assays

Kinetic assays were carried out by measuring the appearance of the product in the reaction medium in an UV–visible PerkinElmer Lambda-2 spectrophotometer, on-line interfaced with a PC Intel-486 DX-66 microcomputer. Temperature was maintained at 25 °C using a Haake D1G circulating waterbath with a heater/cooler and checked using a Cole-Parmer digital thermometer with a precision of ± 0.1 °C. Reference cuvettes contained all the components except the substrate, with a final volume of 1 ml.

The monophenolase and diphenolase activities of mushroom tyrosinase were determined spectrophotometrically by using MBTH, which is a potent nucleophile through its amino group which attacks the enzyme-generated *o*-quinones [25]. This assay method is highly sensitive, reliable and precise [21,22,25]. MBTH traps the enzyme-generated *o*-quinones to render a soluble MBTH-quinone adduct with high molar absorptivity. MBTH-quinone adducts were soluble and stable at acidic pH, whereas at pH 6.8 (the optimum pH for mushroom tyrosinase), these adducts were soluble and evolved to show an isosbestic point. The stability of the MBTH-quinone adducts and the rapid assays provide a reliable method for determining the monophenolase and diphenolase activities of tyrosinase from several sources [22,25].

Diphenolase activity on 4MC and catechol was determined by measuring the disappearance of NADH [14] in rapid kinetic assays. The respective MBTH-quinone adducts were not very

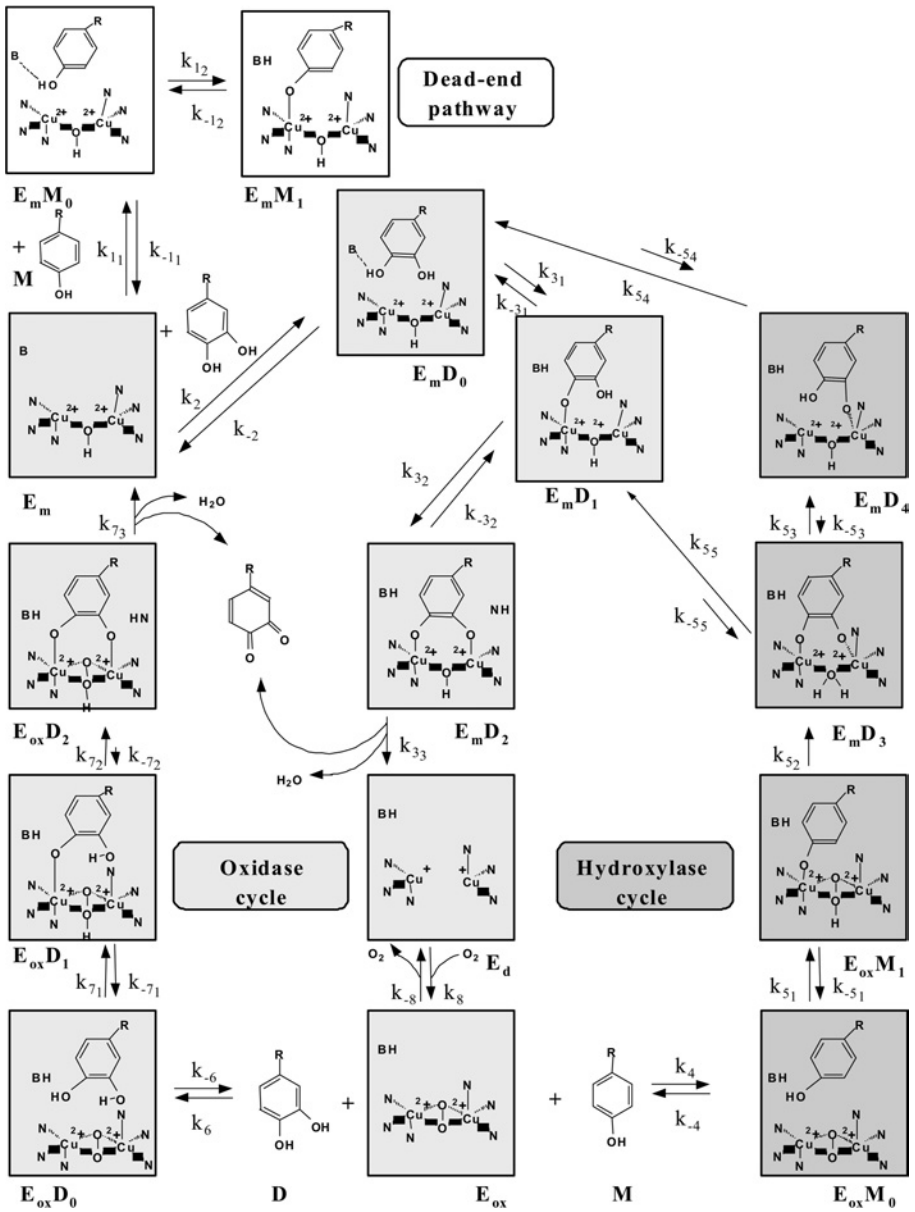

Scheme 2 Structural mechanism proposed for the reaction of tyrosinase with monophenols and *o*-diphenols

E_m, *met*tyrosinase; E_{ox}, *oxy*tyrosinase; E_d, *deoxy*tyrosinase; M, monophenol; D, *o*-diphenol; B, acid–base catalyst. Dead-end pathway: E_mM_0, interaction complex between E_m and M; E_mM_1, nucleophilic attack complex from M to E_m. Diphenolase cycle: E_mD_0, interaction complex between E_m and D; E_mD_1, axial nucleophilic attack complex from the hydroxy group of C-4 on E_m; E_mD_2, diaxial binding complex of D with E_m; $E_{ox}D_0$, interaction complex of D with E_{ox}; $E_{ox}D_1$, axial binding complex of D with E_{ox}; $E_{ox}D_2$, diaxial binding complex of D with E_{ox}. Monophenolase cycle: $E_{ox}M_0$, interaction complex of M with E_{ox}; $E_{ox}M_1$, axial nucleophilic attack complex from M to E_{ox}; E_mD_3, axial–equatorial hydroxylation complex from M to D; E_mD_4, rearrangement complex with C-4 bond break.

soluble and so MBTH was not used as a coupled reagent [26]. Since the *o*-diphenol TBC yielded a highly stable *o*-quinone, the diphenolase activity of tyrosinase on TBC was determined by measuring the appearance of the enzyme-generated *o*-quinone in rapid kinetic assays [27].

Kinetic data analysis

The values of K_m and V_{max} were calculated from triplicate measurements of V_0 for each substrate concentration. The reciprocals of the variances of V_0 were used as weighting factors in the non-linear regression fitting of V_0 against substrate concentration data to the Michaelis–Menten equation [28–30]. The fitting was carried out using Gauss–Newton's algorithm implemented in the Sigma Plot 4 program for Windows (Jandel Scientific, Corte Madera, CA, U.S.A.). Initial estimations of K_m and V_{max} were obtained from the Hanes–Wolf equation, a linear transformation of the Michaelis–Menten equation [29].

Solvent deuterium isotope effect

The solvent deuterium isotope effect on V_{max} and K_m of tyrosinase for the different substrates was determined as a function of the atom fraction of deuterium in the solution. Stock solutions of

Table 1 Proton inventory studies for the oxidation of *o*-diphenols by tyrosinase

Diphenol	Kinetic parameter	δ_3 (p.p.m.)	δ_4 (p.p.m.)	Fractionation factor (Φ^P)	Overall isotope effect (K_H/K_D)
4MC	k_{cat}	146.43	144.06	0.84 ± 0.08	1.19 ± 0.1
	K_m				
DHPPA	k_{cat}	146.51	144.61	0.76 ± 0.07	1.32 ± 0.1
DHPAA	k_{cat}	146.43	144.96	0.67 ± 0.06	1.49 ± 0.1
TBC	k_{cat}	146.24	144.09	0.64 ± 0.06	1.56 ± 0.1
	K_m				
Dopamine	k_{cat}	146.79	145.58	0.63 ± 0.06	1.58 ± 0.1
L-Dopa	k_{cat}	146.92	146.05	0.60 ± 0.06	1.67 ± 0.1
DL-Dopa	k_{cat}	146.92	146.06	0.59 ± 0.05	1.69 ± 0.1
D-Dopa	k_{cat}	146.92	146.06	0.60 ± 0.06	1.67 ± 0.1
Catechol	k_{cat}	146.59	146.59	0.44 ± 0.04	2.27 ± 0.2
	K_m			0.76 ± 0.08	1.32 ± 0.1

sodium phosphate buffer and different substrates in H_2O and ^2H_2O were prepared and combined in various proportions to give different atom fractions (n) of deuterium. ^2H_2O buffers were prepared by freeze-drying the corresponding H_2O buffer and dissolving the solid in ^2H_2O. Enzyme samples were prepared to have the same percentage of ^2H_2O as the reaction mixture by combining stock solutions of enzyme in H_2O and ^2H_2O in the appropriate proportions. Preparing the enzyme in H_2O did not change the value of the deuterium isotope effect on K_m or V_{max}. Thus prior equilibration of the enzyme with the ^2H_2O percentage used in a particular experiment was not necessary.

NMR assays

^{13}C NMR spectra of substrates were obtained at pH 7.0 on a Varian Unity spectrophotometer (300 MHz) using ^2H_2O as solvent. Chemical-shift values (δ) were measured relative to those for tetramethylsilane ($\delta = 0$). The maximum accepted error for each peak was ± 0.03 p.p.m.

RESULTS AND DISCUSSION

It is known that the oxidation of monophenols and *o*-diphenols by tyrosinase involves the transfer of protons, and so a solvent deuterium isotope effect on k_{cat} and K_m is to be expected [20,32–34]. In the present work, the oxidation of monophenols and *o*-diphenols by tyrosinase was studied in $H_2O/^2H_2O$ mixtures in various proportions and, from the measurements of V_0 against $[S]_0$, k_{cat} and K_m were calculated for each atom fraction of deuterium, n, (k_{cat}^{fn}, K_m^{fn}) and related with the experimental value obtained in water ($n = 0$; k_{cat}^{f0}, K_m^{f0}) (Table 1).

Diphenolase activity

Experimental assays: $k_{cat}^{fn}/k_{cat}^{f0}$ against n

The ratio of $k_{cat}^{fn}/k_{cat}^{f0}$ against n for some *o*-diphenols is shown in Figures 1, 2 and 3. This proton inventory plot indicates that k_{cat} is reduced in ^2H_2O. The data best fit a straight line of negative slope with all the *o*-diphenols used. The dependence of $k_{cat}^{fn}/k_{cat}^{f0}$ on n is given by eqn (1) [32]:

$$k_{cat}^{fn}/k_{cat}^{f0} = \frac{\prod_{i}^{v}\left(1 - n + n\Phi_i^P\right)}{\prod_{j}^{v}\left(1 - n + n\Phi_j^R\right)} \quad (1)$$

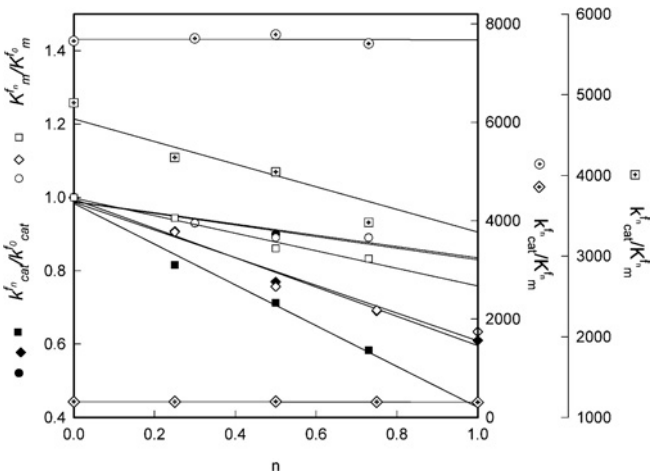

Figure 1 Plots of the ratio of several constants $k_{cat}^{fn}/k_{cat}^{f0}$, K_m^{fn}/K_m^{f0} and $k_{cat}^{fn}/k_{cat}^{f0}$ against *n* for *o*-diphenols: (circles) 4MC, (rhombi) TBC and (squares) catechol

Assay conditions: 0.82 nM tyrosinase, 0.3–7.0 mM TBC, 10 μM–1.2 mM 4MC and catechol and 50 mM sodium phosphate buffer, pH 7.0 at 25 °C. The V_0 values were calculated and then fitted to V_0 against $[D]_0$, to obtain V_{max} and K_m. The k_{cat} was determined from the value of V_{max}.

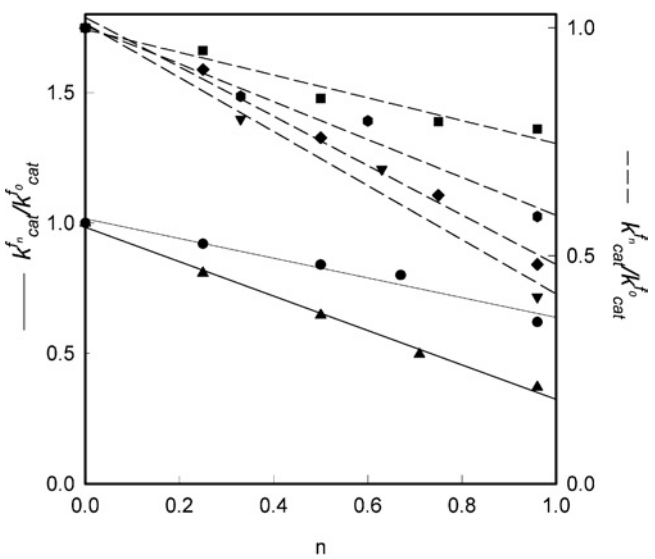

Figure 2 Plots of $k_{cat}^{fn}/k_{cat}^{f0}$ ratio against *n* for monophenols and *o*-diphenols with charge: dopamine (●), tyramine (▲), DHPPA (■), PHPPA (◆), DHPAA (▼) and PHPAA (⬢)

Assay conditions: 50 mM sodium phosphate buffer, pH 7.0 at 25 °C, 2% DMF (*N*,*N*′-dimethylformamide), 2mM MBTH for dopamine/tyramine, 4 mM for DHPPA/PHPPA and DHPAA/PHPAA, and different concentrations of substrate. The enzyme concentrations were 4.92 nM for dopamine, DHPPA and DHPAA, and 49.2 nM for tyramine, PHPPA and PHPAA.

where Φ_i^P and Φ_j^R are the fractionation factors for deuterium in the *i*th site of the product and the *j*th site of the reactant respectively. Thus an isotope fractionation factor for a particular site represents the isotopic free-energy difference at that site compared with the free-energy difference for an average site in bulk water. Since the products take over all the sites which contribute to the solvent isotope effect, the relationship between formation constants and n will, in general, be non-linear (see eqn 1). The linear plots obtained for these *o*-diphenols (Figures 1, 2 and 3) indicates that a single proton is responsible for the isotope effect [19], and that this proton must correspond to one of the phenolic hydroxy

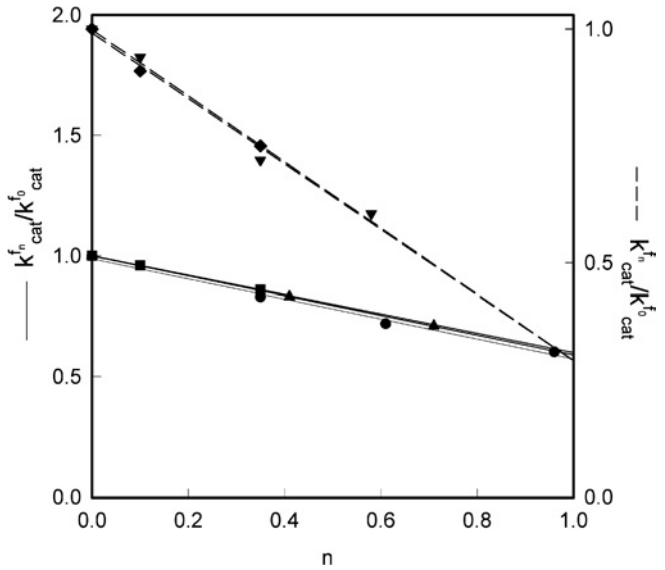

Figure 3 Plots of the $k^{f_n}_{cat}/k^{f_0}_{cat}$ ratio against *n* for isomer monophenols and *o*-diphenols

Assay conditions: 50 mM sodium phosphate buffer, pH 7.0 at 25 °C, 2% DMF (*N*,*N*′-dimethylformamide), 5 mM MBTH and different concentrations of L-dopa (●), DL-dopa (▲), D-dopa (■), L-tyrosine (▼) or DL-tyrosine (◆). The enzyme concentrations were: 4.92 nM for L-dopa, DL-dopa and D-dopa, and 49.2 nM for L-tyrosine and DL-tyrosine.

groups of the *o*-diphenols, since these protons must be released to carry out the oxidation to *o*-quinone. Since the fractionation factor for the substrate must be 1.0 [32], the denominator in eqn (1) is 1, and the equation reduces to:

$$k^{f_n}_{cat}/k^{f_0}_{cat} = 1 - (1 - \Phi^P)n \quad (2)$$

This is represented in Figures 1, 2 and 3, from which the fractionation factor for the proton in the product Φ^P is calculated (Table 1). As has been demonstrated in previous studies [20], the possible proton acceptor in the reaction mechanism of the enzyme can be deduced from this value of Φ^P. The results indicated that one of the different proton transfer steps is more affected by the presence of ^2H_2O than the others, and that this stage must be rate-limiting for the mechanism. We previously suggested [16,17] that the rate-limiting step for the mechanism of Scheme 2 might be that controlled by k_7 (k_{7_1}), which would involve the nucleophilic attack of the oxygen of the hydroxy group in C-4 on the copper atoms of the binuclear site and also proton transfer to the peroxide bound to the E_{ox} form (as might be expected in the case of protonic transfer between oxygen). When a *o*-diphenol is oxidized (see Scheme 2), the fact that $\delta_4 < \delta_3$ indicates that the attack on Cu_A must be initiated by the hydroxy group of C-4. In the E_m form (k_{3_1}), the base B would accept the proton, whereas in the E_{ox} form (k_{7_1}), in which the base is already protonated, the proton would probably be transferred to the peroxide. Since this step is much slower (k_{7_1}), it would be responsible for the isotope effect.

Thus the value of Φ^P depends of the value of δ_4 (note that Φ^P is the ratio $k^{f_n}_{cat}/k^{f_0}_{cat}$ with $n = 1$) and, therefore, a higher value of δ_4 (poorer nucleophilic attack of the oxygen of C-4) leads to lower values of Φ^P, i.e. the isotope effect is greater (Table 1). Note that this occurs in *o*-diphenols without charge, with a positive charge or with a negative charge (Figures 1, 2 and 3 respectively). Moreover, in the case of isomer *o*-diphenols such as L-dopa, DL-dopa and D-dopa, the value of Φ^P is the same since the values of δ_3 and δ_4 are the same (Figure 3).

Experimental assays: $K^{f_n}_m/K^{f_0}_m$ against *n*

We also determined K_m in different atom fractions, *n*, of deuterium for the different *o*-diphenols. The representation of $K^{f_n}_m/K^{f_0}_m$ against *n* differs according to which *o*-diphenol is used. In the case of *o*-diphenols with $R_1 = -CH_3$ or $-CH(CH_3)_2$, such as 4MC and TBC, the representation of $K^{f_n}_m/K^{f_0}_m$ against *n* is linear, and has the same slope as $k^{f_n}_{cat}/k^{f_0}_{cat}$ against *n*. However, in the case of catechol (with $R_1 = -H$), the dependences $K^{f_n}_m/K^{f_0}_m$ and $k^{f_n}_{cat}/k^{f_0}_{cat}$ against *n* have a different slope (Figure 1). This behaviour can be interpreted by taking into account the kinetic analysis of the mechanism of Scheme 1 with $M = 0$ [17]. Thus the analytical expression of k_{cat} and K_m is:

$$k_{cat} = \frac{k_3 k_7}{k_3 + k_7} \quad (3)$$

$$K_m = \frac{k_{cat}(k_2 + k_6)}{k_2 k_6} \quad (4)$$

As demonstrated in a previous study [20], these expressions can be simplified to:

$$k_{cat} = k_7 \quad (5)$$

$$k_m = \frac{k_{cat}}{k_6} \quad (6)$$

In the case of 4MC and TBC, since the slope of $K^{f_n}_m/K^{f_0}_m$ against *n* is equal to that of $k^{f_n}_{cat}/k^{f_0}_{cat}$ against *n* (Figure 1), it is evident that there is no solvent deuterium isotope effect on k_6 (eqn 6) and so:

$$\frac{K^{f_n}_m}{K^{f_0}_m} = \frac{k^{f_n}_{cat}}{k^{f_0}_{cat}} \quad (7)$$

However, this does not occur when the *o*-diphenol used is catechol, when the representation of $K^{f_n}_m/K^{f_0}_m$ against *n* shows a lower slope than the representation of $k^{f_n}_{cat}/k^{f_0}_{cat}$ against *n*. This difference could be explained if k_6 (the binding constant of substrate to E_{ox} form) decreases with increasing concentrations of deuterium in the medium. In this case, $K^{f_n}_m/K^{f_0}_m \neq k^{f_n}_{cat}/k^{f_0}_{cat}$ because $k^{f_n}_6 < k^{f_0}_6$ and thus:

$$\frac{K^{f_n}_m}{K^{f_0}_m} = \frac{k^{f_n}_{cat} k^{f_0}_6}{k^{f_0}_{cat} k^{f_n}_6} \quad (8)$$

This decrease in k_6 with increasing concentrations of ^2H_2O might be explained by the inductive effect of the phenolic hydroxy group on the ring, which would increase the electron density on the ring and improve the interaction with the hydrophobic cavity of the active site of the enzyme. When H is replaced by ^2H, the inductive effect and the interaction with the hydrophobic cavity are less pronounced. Thus the k_6 binding constant decreases and the plot of $K^{f_n}_m/K^{f_0}_m$ against *n* would have a lower slope than the plot of $k^{f_n}_{cat}/k^{f_0}_{cat}$ against *n*. However, in the case of 4MC and TBC, the inductive effect of the R groups (*tert*-butyl and methyl respectively) is so high that the effects of the hydroxy group on the ring are negligible. In this case, the value of k_6 would remain constant even though the hydroxy group was deuterated. This implies that the slopes of the plots of $K^{f_n}_m/K^{f_0}_m$ and $k^{f_n}_{cat}/k^{f_0}_{cat}$ against *n* are the same.

In the case of *o*-diphenols with positive or negative charge, the dependence of $K^{f_n}_m/K^{f_0}_m$ on *n* was not linear and increased (results not shown), probably because hydrogen bonds were established. This would indicate that an increase in *n* produces an increase in $K^{f_n}_m$, because the decrease in k_6 is more pronounced than the

diminution of k_{cat} (see eqn 6), and therefore, in the presence of deuterium, the binding to the enzyme is more difficult. This is possibly due to the presence of R groups with protons that can be substituted by deuterium in the *o*-diphenols and to their influence on the formation of hydrogen bonds with amino acid groups of the enzyme, or between deuterated groups of the enzyme and oxygen of the R groups of the substrate.

In the case of the stereoisomers of the dopa substrate (Figure 3; see Table 1), the isotope effect on k_{cat} is the same, since the values of δ_4 are the same. However, the different values of K_m (results not shown) could be related with the different spatial orientations of the groups bound to the chiral carbon in the substituent R of C-1 [22,35].

From the data of Table 1, it can be seen that in the case of *o*-diphenols, the isotope effect varies between 1.19 and 2.27 for 4MC and catechol respectively. These values and the corresponding fractionation factor values show that, as part of the rate-determining step, a transition-state hydrogen bridge is established between two oxygen atoms and that protons are transferred between them (see Table 3 of [19]). Note that, when the δ_4 value is very low, the hydroxy group oxygen of C-4 is a potent nucleophile, and the limiting step is the nucleophilic attack on the copper, i.e. this type of substrate does not need the assistance of released protons. However, in the case of catechol, which has lower nucleophilic power ($\delta_4 = 146.59$), the isotope effect value (2.27) demonstrated that the nucleophilic attack needs the assistance of the release of the proton, and thus these steps are concerted. Moreover, the existence of different kinetic deuterium effects (1.19–2.27) indicates clearly that the proton transfer is involved in the rate-determining step.

Monophenolase activity

When the monophenolase activity of tyrosinase is studied using different monophenols, the kinetic mechanism of the enzyme undergoes two cycles (hydroxylase and oxidase cycles) with three common intermediates (Scheme 1) [8,11].

Experimental assays: $k_{cat}^{f_n}/k_{cat}^{f_0}$ against *n*

The ratio of $k_{cat}^{f_n}/k_{cat}^{f_0}$ against *n* for monophenols is shown in Figures 2, 3 and 4. These proton inventory plots indicate that k_{cat} is reduced in ^2H_2O, as occurs in the case of *o*-diphenols. The data best fitted a straight line of negative slope in all cases (Figures 2–4). The dependence of $k_{cat}^{f_n}/k_{cat}^{f_0}$ on *n* is also given by eqn (1) [32]. Note that in the mechanism of Scheme 1, when the enzyme acts on monophenols (in the steady-state, it also acts on *o*-diphenols), a total of six protons are transferred (see Scheme 1). As in the case of *o*-diphenols, the rate-limiting step for the mechanism of Scheme 2 is controlled by the substrate reaction with the E_{ox} form of the enzyme, which involves the nucleophilic attack of the hydroxy group oxygen of C-4 on the Cu_A atoms of the binuclear site and proton transfer to the peroxide bound to the E_{ox} form controlled by k_{5_1} and, in addition, the electrophilic attack on the benzene ring controlled by k_{5_2}. Therefore the lower the electronic density in C-4 (higher value of δ_4), the higher the isotope effect (lower value of Φ^P) (Table 2).

Note that, in the case of some monophenols, which always show higher δ_4 values than *o*-diphenols, the Φ^P value is higher than for the *o*-diphenols, as is the case with 4HA (Tables 1 and 2). These results could be explained by taking into account that monophenol hydroxylation involves two steps (Scheme 2): the nucleophilic attack of the hydroxy group oxygen of C-4 on Cu_A, controlled by k_{5_1}, and the electrophilic attack of the peroxide group of the C-3 position, controlled by k_{5_2}. The kinetic analysis of the monophenolase activity [16] shows that:

$$k_{cat}^{M} = \frac{k_{5_1} k_{5_2}}{k_{5_1} + k_{5_2}} \quad (9)$$

and

$$k_m^{M} = \frac{k_{cat}^{M}}{k_{+4}} \quad (10)$$

In the case of monophenols with low δ_4 values, the nucleophilic attack step (k_{5_1}) may be faster than the electrophilic attack step (k_{5_2}), $k_{5_1} > k_{5_2}$ [36], in which case the isotope effect will be small or near null, and the Φ^P value high (see Table 2). When the δ_4 value increases, the nucleophilic attack step is limiting, $k_{5_1} < k_{5_2}$, and the isotope effect is higher (lower Φ^P). In the case of *m*-hydroxylated substrates, this effect is observed when they are compared with the *p*-hydroxylated isomers. In *m*-monophenols, the isotope effect is greater (small Φ^P) because $\delta_3^m > \delta_4^m$, and thus the nucleophilic

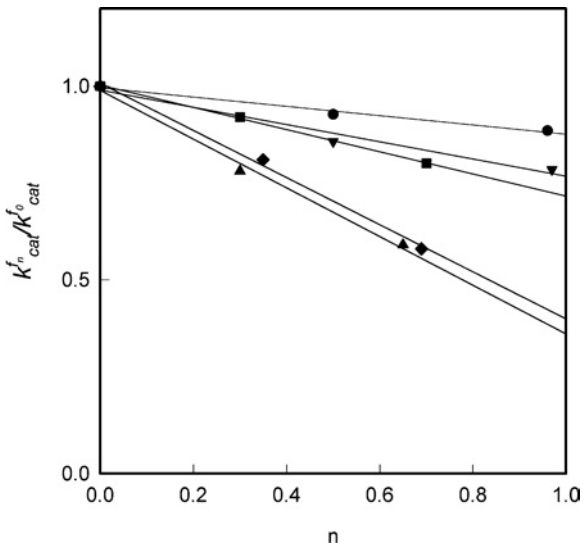

Figure 4 Plots of the ratio of several constants $k_{cat}^{f_n}/k_{cat}^{f_0}$ against *n* for *p*- and *m*-monophenols

Assay conditions: 50 mM sodium phosphate buffer, pH 7.0 at 25 °C, 2% DMF (*N*,*N*′-dimethylformamide), 2.5 mM MBTH, and different concentrations of 4EP (▼), 4HA (●), 3HA (▲), 4HBA (■) or 3HBA (◆). The enzyme concentrations were 4.92 nM for 4HA, 24.6 nM for 4EP and 4HBA, and 98.4 nM for 3HA and 3HBA.

Table 2 Proton inventory studies for the oxidation of monophenols by tyrosinase

Monophenol	Kinetic parameter	δ_3 (p.p.m.)	δ_4 (p.p.m.)	Fractionation factor (Φ^P)	Overall isotope effect (K_H/K_D)
4HA	k_{cat}	118.9	152.29	0.88 ± 0.08	1.14 ± 0.1
4EP	k_{cat}	119.01	152.39	0.78 ± 0.07	1.43 ± 0.1
4HBA	k_{cat}	116.54	156.63	0.71 ± 0.07	1.41 ± 0.1
PHPAA	k_{cat}	118.05	156.49	0.50 ± 0.05	2.00 ± 0.2
PHPPA	k_{cat}	118.02	156.13	0.46 ± 0.04	2.17 ± 0.2
3HBA	k_{cat}	158.44	117.41	0.39 ± 0.04	2.56 ± 0.2
3HA	k_{cat}	159.49	110.97	0.37 ± 0.04	2.70 ± 0.2
Tyramine	k_{cat}	118.49	157.28	0.34 ± 0.03	2.94 ± 0.3
L-Tyrosine	k_{cat}	118.08	158.86	0.29 ± 0.03	3.45 ± 0.3
DL-Tyrosine	k_{cat}	118.08	158.86	0.30 ± 0.03	3.33 ± 0.3

attack step is more limiting and needs the assistance of proton release (Figure 4). Note that monophenolic stereoisomers, such as L-tyrosine and DL-tyrosine, show the same value of Φ^P, since both have the same values of δ_3 and δ_4 (Table 2; Figure 3). These results are in accordance with theoretical studies carried out with oxyhaemocyanin [37].

Table 2 shows that, in the monophenols studied, the isotope effect varies between 1.14 and 3.33, indicating that proton transfer from the hydroxy group on C-4 is involved in the rate-limiting step. Taking into account the Φ^P values (see also Table 1 of [19]), it can be deduced that in the rate-limiting step of monophenols, a transition-state hydrogen bridge between two oxygen atoms is probably established.

Note that for monophenols with low δ_4 values (but much higher than that of any diphenol), the isotope effect is minimal, as occurs with 4HA. In this case (Scheme 2), although the nucleophilic attack needs the assistance of proton release, the rate-limiting step could be the electrophilic attack on the benzene ring. As the δ_4 value increases (see Table 2), so the nucleophilic nature of the hydroxy group oxygen decreases, so that it needs the assistance of proton release, and the isotope effect increases (tyrosine, $\delta_4 = 158.86$ and $K_H/K_D = 3.33$; Table 2).

Experimental assays: $K_m^{f_n}/K_m^{f_0}$ against n

The value of K_m in different atom fractions, n, of deuterium was also determined for the different monophenols. The plot of $K_m^{f_n}/K_m^{f_0}$ against n was non-linear and increased for all the monophenols (results not shown), indicating that, as in *o*-diphenols, the hydrogen bonds are established when the R group of C-1 makes it possible. The analytical expression for K_m^M (eqn 10) indicates that k_{+4} (the binding constant) decreases more than k_{cat}^M and so K_m^M increases in the presence of ^2H_2O, because hydrogen bonds are difficult to forge.

Conclusion

To summarize, when ^2H_2O is used as solvent, an isotope effect is evident in the oxidation of monophenols and *o*-diphenols by tyrosinase. The experimental results confirm that one of the different proton transfer steps is more affected by the presence of ^2H_2O than the others (Tables 1 and 2). The nucleophilic attack of the hydroxy group oxygen of C-4 on the Cu_A of the binuclear site of the E_{ox} form, assisted by proton transfer to the peroxide group (k_{7_1} diphenols, k_{5_1} monophenols), is rate-limiting for the reaction mechanism (Scheme 2). Therefore a high value of δ_4 (low electron density of the hydroxy group oxygen of C-4) implies the strong assistance of proton release and a similarly strong isotope effect (Tables 1 and 2). Note that diphenolase activity (oxidase cycle) involves four protons, whereas monophenolase activity (hydroxylase and oxidase cycles) involves six protons (Scheme 2).

This work was supported in part by grants from the MCYT (Ministerio de Ciencia y Tecnologia) (Spain) Project AGL2002-01255 ALI and from the Fundación Séneca/Consejería de Agricultura, Agua y Medio Ambiente (Murcia) Project AGR/10/FS/02. L. G. F. has a fellowship from the University of Murcia.

REFERENCES

1 Prota, G., d'Ischia, M. and Napolitano, A. (1998) The chemistry of melanins and related metabolites. In The Pigmentary System, Physiology and Pathology (Nordlund, J. J., Boissy, R. E., Hearing, V. J., King, R. A. and Ortonne, J. P., eds.), pp. 307–332, Oxford University Press, Oxford
2 Nicolas, J. J., Richard-Forget, F., Goupy, P. M., Amiot, M. J. and Aubert, S. (1994) Enzymatic browning reactions in apple products. Crit. Rev. Food Sci. **34**, 109–157
3 Zawistowski, J., Biliaderis, C. G. and Eskin, N. A. M. (1991) Polyphenol Oxidase. In Oxidative Enzymes in Foods (Robinson, D. S. and Eskin, N. A. M., eds.), pp. 217–273, Elsevier Science, London
4 Van Gelder, C. W. G. and Flurkey, W. A. J. (1997) Sequence and structural features of plant and fungal tyrosinases. Phytochemistry **45**, 1309–1323
5 Mason, H. S. (1956) Structure and functions of the phenolase complex. Nature (London) **177**, 79–81
6 Sánchez-Ferrer, A., Rodríguez-López, J. N., García-Cánovas, F. and García-Carmona, F., (1995) Tyrosinase: a comprehensive review of its mechanism. Biochim. Biophys. Acta **1247**, 1–11
7 García-Cánovas, F., García-Carmona, F., Vera-Sánchez, J., Iborra, J. L. and Lozano, J. A. (1982) The role of pH in the melanin biosynthesis pathway. J. Biol. Chem. **257**, 8738–8744
8 Rodríguez-López, J. N., Tudela, J., Varón, R., García-Carmona, F. and García-Cánovas, F. (1992) Analysis of a kinetic model for melanin biosynthesis pathway. J. Biol. Chem. **267**, 3801–3810
9 Yong, G., Leone, O. and Strothkamp, K. G. (1990) *Agaricus bisporus* metapotyrosinase: preparation, characterization, and conversion to mixed-metal derivatives of the binuclear site. Biochemistry **29**, 9684–9690
10 Jolley, Jr, R. L., Evans, L. H., Makino, N. and Mason, H. S. (1974) Oxytyrosinase. J. Biol. Chem. **249**, 335–345
11 Solomon, E. I., Sundaram, U. M. and Machonkin, T. E. (1996) Multicopper oxidases and oxygenases. Chem. Rev. **96**, 2563–2605
12 Ros, J. R., Rodríguez-López, J. N. and García-Cánovas, F. (1994) Tyrosinase: kinetic analysis of the transient phase and the steady state. Biochim. Biophys. Acta **1204**, 33–42
13 Ros, J. R., Rodríguez-López, J. N. and García-Cánovas, F. (1993) Effect of L-ascorbic acid on the monophenolase activity of tyrosinase. Biochem. J. **295**, 309–312
14 Espín, J. C., Varon, R., Fenoll, L. G., Gilabert, M. A., García-Ruiz, P. A., Tudela, J. and García-Cánovas, F. (2000) Kinetic characterization of the substrate specificity and mechanism of mushroom tyrosinase. Eur. J. Biochem. **267**, 1–11
15 Fenoll, L. G., Rodriguez-Lopez, J. N., García-Sevilla, F., Tudela, J., García-Ruiz, P. A., Varon, R. and García-Cánovas, F. (2000) Oxidation by mushroom tyrosinase of monophenols generating slightly unstable *o*-quinones. Eur. J. Biochem. **267**, 1–15
16 Fenoll, L. G., Rodríguez-López, J. N., García-Sevilla, F., García- Ruiz, P. A., Varón, R., García-Cánovas, F. and Tudela, J. (2001) Analysis and interpretation of the action mechanism of mushroom tyrosinase on monophenols and diphenols generating highly unstable *o*-quinones. Biochim. Biophys. Acta **1548**, 1–22
17 Rodriguez-Lopez, J. N., Fenoll, L. G., García-Ruiz, P. A., Varon, R., Tudela, J., Thorneley, R. N. and García-Cánovas, F. (2000) Stopped-flow and steady-state study of the diphenolase activity of mushroom tyrosinase. Biochemistry **39**, 10497–10506
18 Conrad, J. S., Dawson, S. R., Hubbard, E. R., Meyers, T. E. and Strothkamp, K. G. (1994) Inhibitor binding to the binuclear active site of tyrosinase: temperature, pH, and solvent deuterium isotope effects. Biochemistry **33**, 5739–5744
19 Venkatasuban, K. S. and Schowen, R. L. (1984) The proton inventory technique. Crit. Rev. Biochem. **17**, 1–44
20 Peñalver, M. J., Rodríguez-López, J. N., García-Ruiz, P. A., García-Cánovas, F. and Tudela, J. (2003) Solvent deuterium isotope effect on the oxidation of *o*-diphenols by tyrosinase. Biochim. Biophys. Acta **1650**, 128–135
21 Rodríguez-López, J. N., Escribano, J. and García-Cánovas, F. (1994) A continuous spectrophotometric method for the determination of monophenolase activity of tyrosinase using 3-methyl-2-benzothializone hydrazone. Anal. Biochem. **216**, 205–212
22 Espín, J. C., García-Ruiz, P. A., Tudela, J. and García-Cánovas, F. (1998) Study of the stereospecificity in mushroom tyrosinase. Biochem. J. **331**, 547–551
23 Duckworth, H. W. and Coleman, J. E. (1970) Physicochemical and kinetic properties of mushroom tyrosinase. J. Biol. Chem. **245** 1613–1625
24 Bradford, M. M. (1976) A rapid and sensitive method for the quantification of microgram quantities of proteins utilizing the principle of protein-dye binding. Anal. Biochem. **72**, 248–256
25 Winder, A. J. and Harris, H. (1991) New assays for the tyrosine hydroxylase and dopa oxidase activities of tyrosinase. Eur. J. Biochem. **198**, 317–326
26 Espín, J. C., Morales, M., Varón, R., Tudela, J. and García-Cánovas, F. (1996) A continuous spectrophotometric method for determining the monophenolase and diphenolase activities of pear polyphenol oxidase. J. Food Sci. **61**, 1177–1201
27 Ros, J. R., Rodríguez-López, J. N., Varón, R. and García-Cánovas, F. (1994) Kinetics study of the oxidation of 4-tert-butylphenol by tyrosinase. Eur. J. Biochem. **222**, 449–452
28 Draper, N. R. and Smith, H. (1981) Applied Regression Analysis, Wiley, New York
29 Endrenyi, L. (1981) Kinetic Data Analysis: Design and Analysis of Enzyme and Pharmacokinetics Experiments, Plenum Press, New York

30 Marquardt, D. W. (1963) An algorithm for least-squares estimation of non-linear parameters. J. Soc. Ind. Appl. Math. **11**, 431–441
31 Reference deleted
32 Schowen, K. B. and Schowen, R. L. (1982) Solvent isotope effects on enzyme systems. Methods Enzymol. **87**, 551–606
33 Schowen, R. L. (1977) In Isotope Effects on Enzyme-Catalyzed Reactions (Cleland, W. W., O'Leary, M. H. and Northrop, D. B., eds.), pp. 64–99, University Park Press, Baltimore
34 Albery, J. (1975) In Proton-Transfer Reactions (Caldin, E. and Gold, V., eds.), pp. 263–315, Wiley & Sons, New York
35 Espín, J. C., García-Ruiz, P. A., Tudela, J. and García-Cánovas, F. (1996) Study of stereospecificity in pear and strawberry polyphenol oxidases. J. Food Sci. **46**, 2469–2473
36 Fenoll, L. G., Rodríguez-López, J. N., Varón, R., García-Ruiz, P. A., García-Cánovas, F. and Tudela, J. (2000) Action mechanism of tyrosinase on *meta*- and *para*-hydroxylated monophenols. Biol. Chem. **381**, 313–320
37 Eisenstein, O., Geissner-Prettre, C., Maddaluno, J., Stussi, D. and Weber, J. (1992) Theoretical study of *oxy*hemocyanin active site: a possible insight on the first step of phenol oxidation of tyrosinase. Arch. Biochem. Biophys. **296**, 247–255

Received 23 January 2004; accepted 17 March 2004
Published as BJ Immediate Publication 17 March 2004, DOI 10.1042/BJ20040136